A Novel MRI-Based Approach to Peripheral Refraction and Prediction of Myopia Progression

SANDER C.M. KNEEPKENS, LUC VAN VUGHT, JAN ROELOF POLLING, CAROLINE C.W. KLAVER, J. WILLEM L. TIDEMAN, AND JAN-WILLEM M. BEENAKKER

• PURPOSE: Optical solutions that create peripheral myopic defocus in the presence of a clear central image have shown to be effective as myopia treatment. This study investigates whether peripheral refraction measured via MRI and ray tracing can predict myopia progression in children.

• METHODS: A total of 1635 children from the Generation R Study, a population-based birth cohort in Rotterdam, the Netherlands, underwent T2 weighted MRI scanning at age 9 years. At both ages 9 and 14 years, ocular biometry, and cycloplegic autorefraction were assessed. Retinal curvature radii were computed from MRI segmentations using semi-automated, customized image processing algorithms. Individual peripheral refraction profiles were modelled through ray tracing. Horizontal and vertical peripheral refraction was analysed at 50-degrees eccentricity. Relative peripheral refraction (RPR) was calculated by subtracting peripheral refraction from central cycloplegic refraction. Yearly myopia progression was calculated and stratified into quantiles (ΔAL), and the effect of RPR on the quantile outcomes was examined using ordinal regression analyses. Predictive performance of RPR on development of myopia was evaluated using ROC-analysis (fast vs slow progressors) and a logistic regression (incident myopia).

• RESULTS: At age 9 years, 207/1635 (13%) children had developed myopia. Myopic children had a significantly more hyperopic RPR compared to emmetropic children at all horizontal eccentricities (–1.8 ± 1.8D vs. 0.2 ± 2.1D) and vertical eccentricities (–1.0 ± 1.9D vs. 0.8 ± 2.2D). Higher vertical (OR: 1.08, CI: 1.02-1.14) and horizontal RPR (OR: 1.16, CI: 1.10-1.22) was associated with faster AL progression. Each diopter increase in vertical RPR (OR: 1.10, CI: 1.01-1.20) and horizontal RPR (OR: 1.23, CI: 1.13-1.35) was associated with an increased risk of incident myopia. ROC analysis indicated that RPR had a maximum predictive AUC of 0.77 for identifying fast progressors. Furthermore, MRI data revealed significant interindividual variations in retinal curvature (SD 1 mm), which resulted in clinically relevant peripheral refractive differences exceeding 8D among children with similar axial length and central SE, suggesting that standard defocus strategies may require individualization.

• CONCLUSIONS: Using this novel approach to calculate peripheral refraction, we provide evidence based on eye shape that peripheral hyperopic refractive error is more pronounced in myopic children and is strongly associated with myopia progression. The significant anatomical variability in retinal radii underscores the need for personalized treatment strategies, which may enhance the efficacy of optical interventions for myopia management. (Am J Ophthalmol 2025;278: 239–249.

AJO.com Supplemental Material available at AJO.com.

This invited article was submitted as part of the Virtual Special Issue on the International Myopia Conference (IMC).
Accepted for publication June 6, 2025.

Department of Ophthalmology (S.K., J.P., C.K., J.T.), Erasmus University Medical Center, Rotterdam, The Netherlands; The Generation R Study Group (S.K., C.K., J.T.), Erasmus University Medical Center, Rotterdam, The Netherlands; Department of Ophthalmology (LV, JB), Leiden University Medical Center, Leiden, the Netherlands; Department of Radiology (L.V., J.B.), Leiden University Medical Center, Leiden, the Netherlands; Department of Ophthalmology (J.T.), St. Martini Hospital, Groningen, The Netherlands; Institute of Molecular and Clinical Ophthalmology (C.K.), Basel, Switzerland; Department of Ophthalmology (C.K.), Radboud University Medical Center, Nijmegen, The Netherlands; Department of Radiation Oncology (JB), Leiden University Medical Center, Leiden, The Netherlands; HollandPTC (J.B.), Delt University of Technology, Delft, The Netherlands

Inquiries to S.C.M. Kneepkens and C.C.W. Klaver Department of Ophthalmology, Erasmus University Medical Center, Rotterdam, The Netherlands; e-mail: s.kneepkens@erasmusmc.nl, c.c.w.klaver@erasmusmc.nl

INTRODUCTION

Myopia prevalence is increasing globally, with projections estimating that by 2050, half of the world population will be myopic and 10% highly myopic.[1,2] Although similar trends are observed across different ethnicities, the prevalence is currently the highest in Asian people. In Europe, the prevalence of myopia is approximately 47% in young adults, whereas in Hong-Kong, a prevalence of 61.5% is already reached at the age of 12. In

0002-9394/$36.00
https://doi.org/10.1016/j.ajo.2025.06.013

Taiwan, the prevalence has even approached 86% in young adults.[3-5]

Measures that can be taken to prevent the development of myopia or reduce progression can be grouped into 3 categories: (1) lifestyle interventions aimed to reduce near work and increase outside exposure; (2) pharmacological interventions with atropine; and (3) optical interventions.[6]

Optical interventions are based on the concept that hyperopic peripheral defocus contributes to myopia, while myopic peripheral defocus may slow or prevent the trait. This concept was first mentioned by Hoogerheide et al. in 1972, though the interpretation of their findings was debated.[7] Subsequent studies have confirmed that myopic children have more hyperopic relative peripheral refraction (RPR) compared to their peers.[8,9] Based on this observation, optical interventions such as specialized spectacle and contact lens designs aim to induce myopic defocus on the peripheral retina while preserving clear central vision[10] A recent study suggested that some optical interventions have limited effects on RPR, possibly due to a reduction in peripheral retinal contrast rather than a true shift in peripheral refraction.[11] Similarly, several longitudinal studies in children did not find a direct relationship between peripheral hyperopia and increased risk of myopia or myopia progression.[9,12,13]

Most current studies determine peripheral refraction by modifying auto-refraction, asking patients to gaze at an off-axis fixation target. However, since auto-refractors are optimized for central vision, their accuracy for peripheral measurements is questionable. This method can be affected by patient compliance issues and off-axis ocular optics, potentially introducing measurement bias.[14,15]

An alternative approach to measurement of peripheral refraction is ray tracing, which calculates light propagation through models of the eye based on subject-specific anatomical parameters.[16] Ray tracing is widely used in refractive surgery for design and selection of intraocular lens implants, but is increasingly being applied to determine peripheral refraction profiles.[17-25] Unlike off-axis autorefractor methods, ray tracing is not affected by fixation errors or optical distortions. However, its result relies on the anatomical correctness of the used eye models. This includes a anatomically correct retinal shapes, which are challenging to measure with conventional ophthalmic instruments.

Recent advances in magnetic resonance imaging (MRI) now allow for quantification of retinal shape using standard clinical MRI-scans.[18,26-28] In this study, we integrate subject-specific ray tracing with MRI to investigate the relationship between relative peripheral refraction and myopia in children. Specifically, we aim to investigate the association between peripheral refraction and changes in SER and axial length growth.

METHODS

• **STUDY POPULATION:** Participants were children from the Generation R study, a population based prospective cohort study of pregnant woman and their children in Rotterdam, the Netherlands. The complete methodology for the Generation R study has been described elsewhere.[29,30] In brief, children visited the research center for detailed examinations at approximately 4-year intervals. At the age 9 visit, a total of 5,862 participants attended, of whom 3,637 (62%) underwent both T2-weighted MRI scans of the right- eye and ophthalmological examinations. Exclusion criteria for the current analysis included poor-quality MRI scans (N = 495), absence of cycloplegic refractive error measurements (N = 1322), absence of axial length measurements (N = 161), and missing covariate data (N = 9). This resulted in a final analysis sample of 1,635 participants (Figure 1). Follow up ophthalmological examinations were completed by 82% (1346/1635) of participants.

The Generation R study protocol was approved by the Medical Ethical Committee of the Erasmus Medical Centre, Rotterdam (MEC 217.595/2002/20). All participants provided written informed consent following the Declaration of Helsinki to participate in the study and consent for data collection from their treating physicians.

• **OPHTHALMOLOGICAL EXAMINATIONS:** Ophthalmological examinations were conducted at age 9 and 13 years old. Ocular biometry measures were obtained using the Zeiss IOL-master 500 (Carl Zeiss MEDITEC IOL-master, Jena, Germany). Axial length (AL) was measured 5 times and the mean axial length for the right eye was calculated. Three keratometry measurements (K1 and K2) of the right eye were averaged and used to calculate mean corneal radius of curvature (CR). Automated cycloplegic autorefraction was performed using Retinomax-3 (Bon, Lübeck, Germany). Cycloplegia was achieved by administering 2 drops of 1% cycloplentolate (3 drops in case of dark irises) spaced 5 minutes apart at least 30 minutes before refractive error measurement. Spherical equivalent (SE) refractive error was calculated as the average sphere +1/2 cylinder. Participants were grouped by refractive error categories based on SE: emmetropia ($-0.5D<SE<+2D$), hyperopia ($SE\geq+2D$), myopia ($SE\leq-0.5D$), high myopia ($SE\leq-6D$). Yearly myopia progression (ΔSE or ΔAL) was calculated by subtracting SE and AL at age 9 from SE and AL at age 13 divided by the number of years between the visits.

• **MAGNETIC RESONANCE IMAGING AND RETINAL SHAPE DETERMINATION:** At 9 years old, participants underwent a 3 Tesla brain MRI scan (Discovery 750, General Electric, Milwaukee, WI, USA) with an 8-channel receive-only head coil.[32] Of the 3637 acquired scans, 2963 (81.5%) were of sufficient quality. Retinal and lens contours were automatically segmented as described by Kneepkens et al.[26] Using these segmentations, the horizontal and vertical retinal radii of curvature and conic constant were computed using an in-house developed python script (version 3.7.10). To

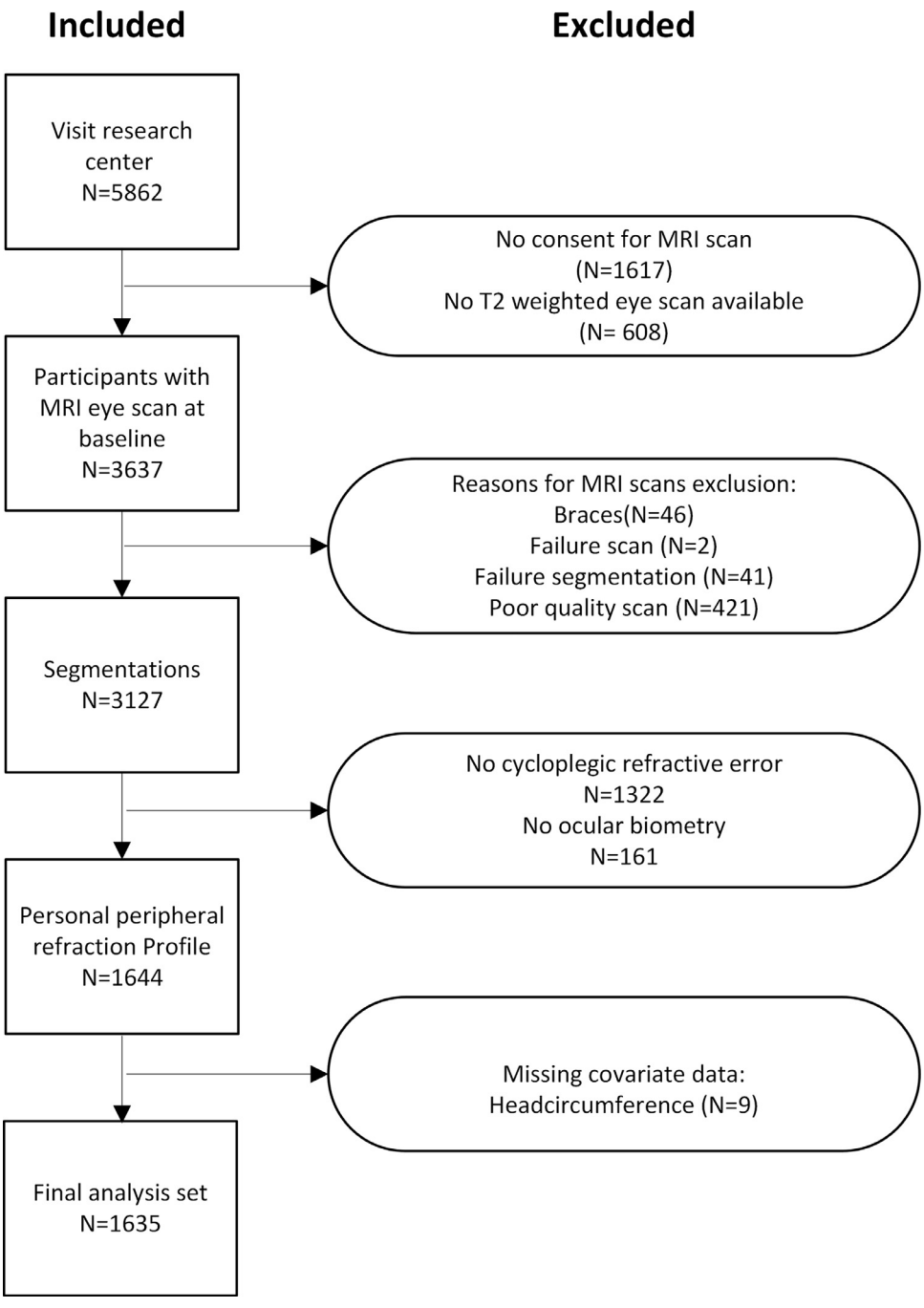

FIGURE 1. Flow chart of study participants.

correct for a potential head tilt, the centres of the vitreous of both eyes were used as reference points. The central horizontal and vertical retinal contours were extracted, and ellipses were fitted through the central 220 degrees of the retina, as described by van Vught et al.[18,31,32] (Figure 2A).

• **PERSONALIZED RAY TRACING:** Subject-specific ray tracing simulations were performed in OpticStudio (version 20.3.2, Ansys inc.) using ZOSPy 1.1.2.[22] A personalized eye model was created for each subject as described by Haasjes et al.[16] In brief, the anterior and posterior cornea curvatures of the Navarro wide-angle eye-model were adapted based on keratometry measurements, while the anterior chamber depth and axial length were obtained from biometry.[33] The crystalline lens model was based on the average lens of a 9-year-old subject,[34] with adjustments to thickness, posterior radius of curvature, and asphericity to match the subject's cycloplegic refractive error. The retina

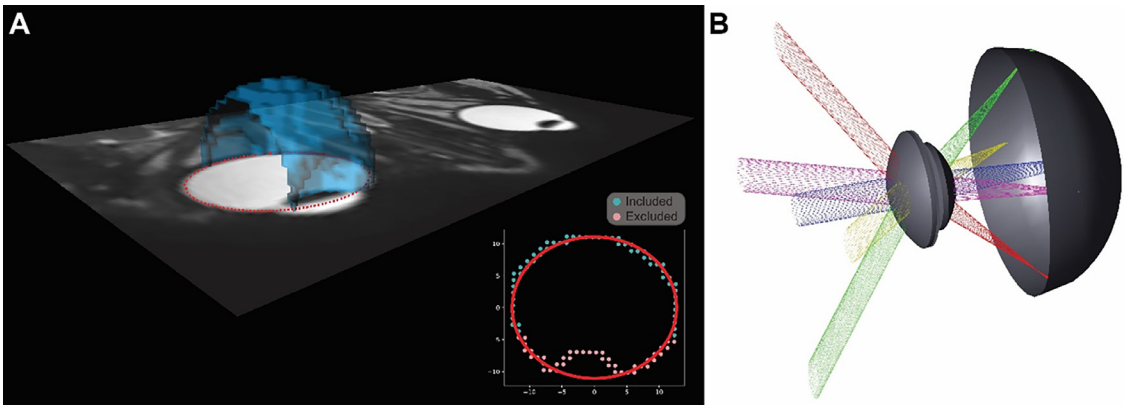

FIGURE 2. A. 3D overlay of the segmented retinal structure (blue) on the MR-image, with an ellipse (red line) fitted through the retinal contour based on the included data points (green dots). Excluded data points are shown in red; B. 3D representation of ray tracing, demonstrating light paths through various points on the eye.

was modelled as biconic surface based on the ellipsoid fit on the MRI-data as described above. The pupil diameter was set to 3.0 mm and the wavelength was set to 589.3 nm.[22,35,36] The full methodology for generation personalized eye models is publicly available at ZOSPy's GitHub repository.[37] Wavefront aberration profiles were obtained for each eye through raytracing simulations, covering visual field angles up to 55 degrees in both the horizontal and vertical direction in steps of 1 degree. (Figure 2B) These profiles were subsequently converted to spherical equivalent of refraction (SE)[19]. (Figure 3) Horizontal and vertical peripheral refraction were calculated at 50 degrees eccentricity. Conventional peripheral refraction measurements have been limited to a maximum of 30 degrees due to optical constraints; however, our MRI-based method allowed for more peripheral assessments.[14] To facilitate comparison with the literature, results at 30 degrees have been included in the Supplementary Material. (Supplementary Table 2) Relative peripheral refraction (RPR) was calculated by subtracting central SE from central cycloplegic SE.

• **COVARIATES:** Birth weight was obtained from medical records and hospital registries. At age 9, measurements of head circumference were taken, as well as body height and weight without shoes. Country of birth of the mother and father were determined via a questionnaire and used as a proxy for ethnicity, following methodology developed by Statistic Netherlands.[38] Ethnicity was categorized as European and Non-European.

• **STATISTICAL ANALYSES:** Comparisons between refractive error groups were conducted using Student's unpaired t-test, one-way ANOVA, or chi square test as appropriate. For analyses involving more than 2 groups, post hoc comparisons were performed using Tukey's test. A correlation matrix was constructed to assess the relationships between RPR, retinal curvature, age, sex, AL, birth weight, ethnicity, body height, head circumference, weight, and BMI (Supplementary Figure 1). To account for multiple comparisons, a Bonferroni correction was applied. The relationship between baseline axial length and retinal radius of curvature was further explored by plotting these variables against each other and stratifying them by axial length progression quartiles (Supplementary Figure 2).

The association between RPR and AL was analyzed using a linear regression model corrected for age, sex, birth weight, body height, head circumference, ethnicity, and both the vertical and horizontal retinal radius of curvature. To investigate the association between RPR and myopia progression (ΔSE and ΔAL), linear regression was considered unsuitable as residuals were not normally distributed. Instead, progression rate was categorized into quantiles, and ordinal regression analysis was used correcting for gender, age, sex, ethnicity, axial length, and retinal curvature as vertical and horizontal retinal radius. The association between RPR and incident myopia was examined in participants who were non-myopic at baseline ($N = 968$) using a logistic regression model corrected for time between visits, gender, age, sex, ethnicity, axial length, and retinal curvature as vertical and horizontal retinal radius.

Lastly, Receiver Operating Characteristic (ROC) curve analysis was performed to assess the predictive value of RPR for myopia progression.[39] Logistic regression models were constructed to compare progression subgroups based on axial elongation quartiles, with Area Under the Curve (AUC) values calculated for different models specification: Model 1, Baseline axial length only without confounding variables; Model 2, RPR only; Model 3, Baseline RPR and AL; Model 4, All of the above, plus age, sex, ethnicity and

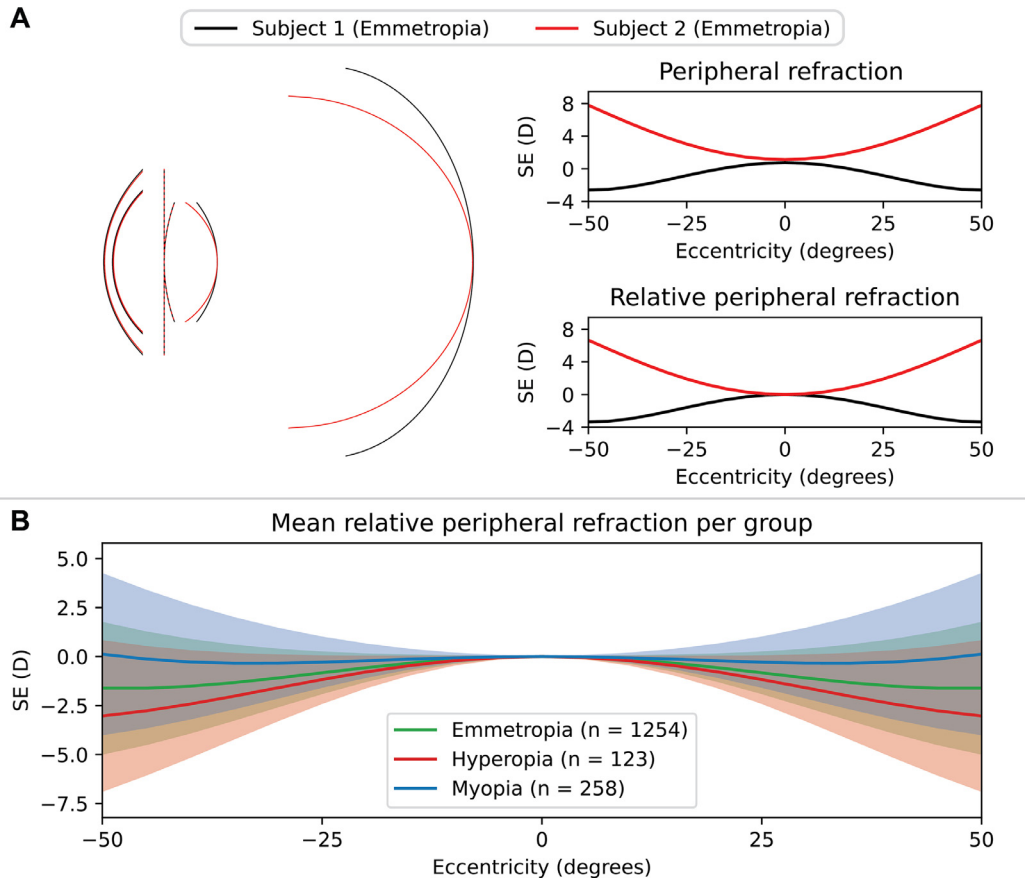

FIGURE 3. A. Peripheral refraction and relative peripheral refraction across eccentricities from 0 to 50 degrees for 2 emmetropes with similar AL but different retinal curvature; B. Group-wise analysis of relative peripheral refraction stratified by refractive error categories, showing the distribution for emmetropia, hyperopia, and myopia. Shaded regions represent the 95% CI.

retinal curvature as potential confounders. To assess multicollinearity, the Variance Inflation Factor (VIF) was calculated for each model, with a values above 4 considered indicative of excessive collinearity. [40]

RESULTS

• **DEMOGRAPHICS:** A total of 1,635 participants (mean age: 9.9 ± 0.4 years) were included in the analysis (Figure 1). Of these, 52% were female, and 70% were of European ancestry. The distribution of refractive error was as follows: 8% (123/1635) hyperopia, 77% (1254/1635) emmetropia, and 16% (258/1635) myopia. Mean SE was 0.6 ± 1.3 D and mean axial length was 23.1 ± 0.8 mm. Average corneal radius was 7.8 ± 0.2mm; average retinal radius was 13.7 ± 1.1mm horizontally and 13.5 ± 1.1mm vertically. Participants excluded from the analysis due to missing covariates were older than those included (10.3 ± 0.7 vs. 9.9 ± 0.4 yrs., $P < .001$), and slightly less likely to be of European ancestry (65% vs. 70%, $P = .05$). No other significant differences were found. (Table 1).

• **PERIPHERAL REFRACTION PROFILE:** Peripheral refraction profiles were compared between hyperopic, emmetropic, and myopic participants (Table 2). Both emmetropes ($P = .006$) and hyperopes ($P = .008$) had a significantly smaller horizontal retinal radius compared to myopes, whereas vertical retinal radius did not differ significantly between groups. Peripheral refractive error (PRE) at 50° eccentricity was significantly lower in myopes compared to emmetropes and hyperopes. Horizontal PRE was –1.5 ± 2.1 D in myopes, significantly lower than –0.2 ± 1.9 D in hyperopes ($P < .001$) and –0.8 ± 1.7 D in emmetropes ($P < .001$). Similar results were found for vertical PRE. Conversely, relative peripheral refraction (RPR) was more hyperopic in myopes; horizontal RPR was 0.2 D in myopes, significantly more hyperopic than –3.1 D in hyperopes ($P < .001$) and -1.6 D in emmetropes ($P < .001$). Similar results were found for vertical RPR (Table 2). Further stratification into smaller SE groups revealed that lower SE was associated with higher RPR (Figure 4). Comparable but

TABLE 1. Baseline Demographics of Study Population Compared to Those Excluded From Analysis

Baseline Characteristics	Study Population (N = 1635)	Excluded Participants (N = 1492)
Mean age, years	9.9 ± 0.4	10.3 ± 0.7**
Girl (%)	52% (847)	50% (748)
European (%)	70%(1150)	65% (968)*
Refractive Error category (%)		(N = 170)
Hyperopic (SE≥+2D)	8% (123)	7% (12)
Emmetropic (–0.5D<SE<+2D)	77% (1254)	77% (131)
Myopic (SE≤-0.5D)	16% (258)	16% (27)
Spherical equivalent (D)	0.6 ± 1.3 D	0.6 ± 1.3 D
Axial length (mm)	23.1 ± 0.8 mm	23.1 ± 0.9 mm
Corneal radius	7.8 ± 0.2mm	7.8 ± 0.3mm
Retinal radius horizontal	13.7 ± 1.1mm	13.8 ± 1.1mm
Retinal radius vertical	13.5 ± 1.1mm	13.5 ± 1.2mm

*P < .05.
**P < .001.

TABLE 2. Peripheral Refractive (PRE) Measures and Relative Peripheral Refraction (RPR) Compared Between Hyperopes, Emmetropes and Myopes.

Peripheral Refractive Error grouped by Refractive Error Categories	Hyperopes (N = 123)	Emmetropes (N = 1254)	Myopes (N = 258)
Axial length	22.3 ± 0.7 mm**	23.4 ± 0.7 mm**	24.4 ± 1.0 mm
Corneal radius	7.8 ± 0.2 mm	7.8 ± 0.3 mm*	7.7 ± 0.3 mm
Horizontal Retinal radius	13.9 ± 1.2mm*	13.8 ± 1.0 mm*	13.5 ± 1.1 mm
Vertical Retinal radius	13.5 ± 1.1mm	13.5 ± 1.1 mm	13.5 ± 1.1 mm
Horizontal PRE 50°	–0.2 ± 1.9 D**	–0.8 ± 1.6 D**	–1.5 ± 2.1 D
Vertical PRE 50 °	0.7 ± 1.7 D**	–0.0 ± 1.8 D**	–1.0 ± 2.1 D
Horizontal RPR 50 °	–3.0 ± 1.9 D**	–1.6 ± 1.7 D**	0.1 ± 2.1 D
Vertical RPR 50 °	–2.2 ± 1.8 D**	–0.9 ± 1.8 D**	0.6 ± 2.2 D

Significance testing was performed using ANOVA with post hoc Tukey analysis comparing Hyperopes and emmetropes to myopes.
*$P < .05$.
**$P < .001$.

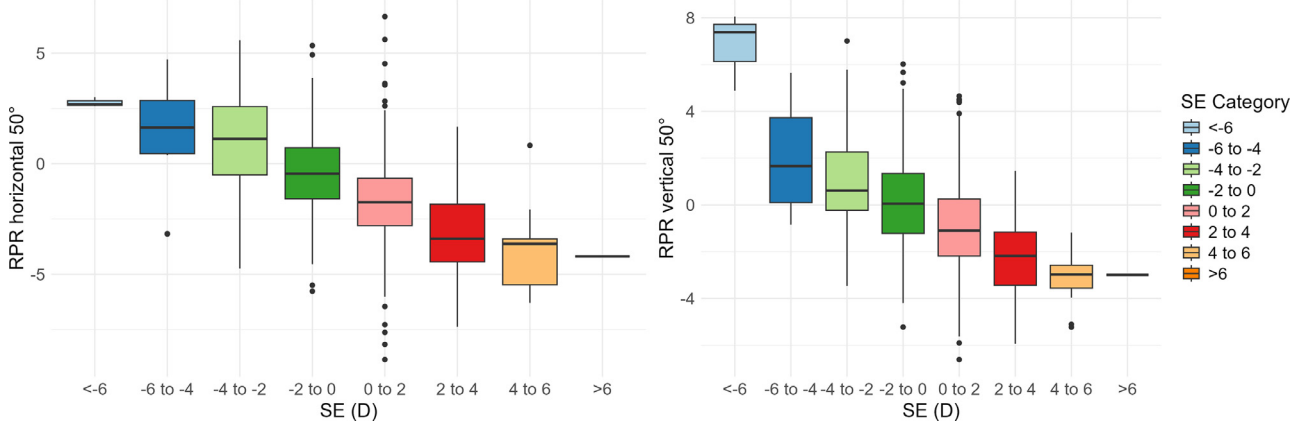

FIGURE 4. Relative peripheral refraction (RPR) at 50° eccentricity grouped by central spherical equivalent.

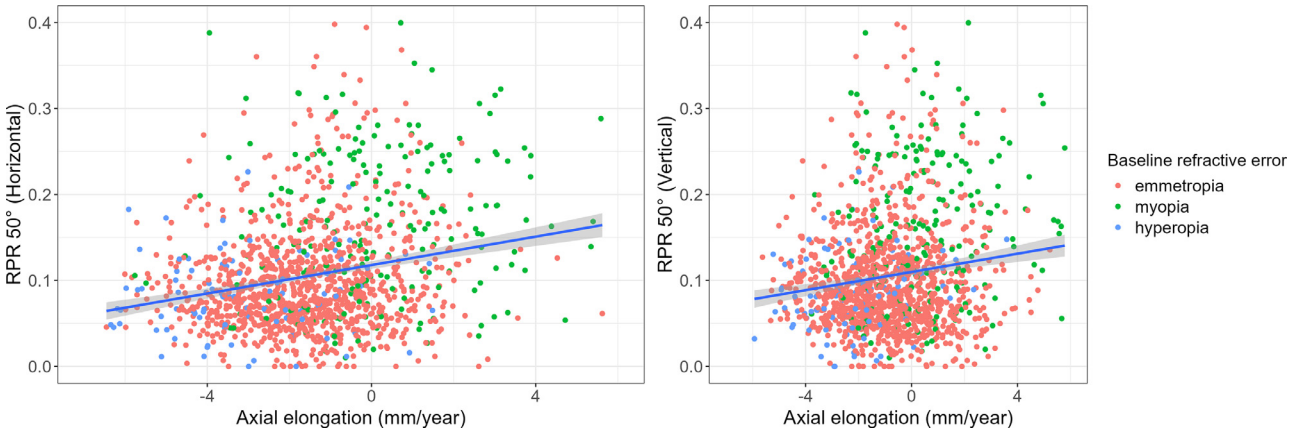

FIGURE 5. Scatter plot showing the relationship between relative peripheral refraction (RPR) at 50° eccentricity in both horizontal (left) and vertical (right) meridians at baseline and axial elongation (mm/year) between age 9 and 13 years. The blue lines represent the best-fit linear regression lines without correction. Emmetropes are indicated in red dots, myopes in green dots, and hyperopes in blue dots.

smaller differences were observed at 30° eccentricity (Supplementary Figure 3 & Supplementary Table 1).

• **FEATURES ASSOCIATED WITH RELATIVE PERIPHERAL REFRACTION:** Regression analysis was conducted for RPR at 50° eccentricity, where the largest differences between groups were found. Results for other eccentricities are provided in Supplementary Table 2. Multivariate linear regression analysis revealed that both horizontal and vertical RPR were significantly associated with AL (β:0.79D/mm, $P < .001$; β:0.95 D/mm, $P < .001$), birth weight (β:-0.16D/kg, $P : .003$; β:-0.18D/kg,$P < .001$), and horizontal retinal radius of curvature (β:-1.42D/mm, $P < .001$; β:-0.17D/mm, $P < .001$). In contrast, vertical retinal radius of curvature was significantly associated only with vertical RPR (β:-1.28D/mm, $P < .001$). With respect to multicollinearity, all predictor variables had VIF values below the common threshold of 4, indicating that this was not a concern.

• **MYOPIA PROGRESSION:** Follow-up ophthalmological data were available for 82% of participants (1346/1635) and were used to assess myopia progression.. Fast progressors (FP; highest quartile) progressed on average 0.21 (range: 0.13-0.50) mm/year, whereas slow progressors (SP; slowest quartile) progressed on average 0.04 (range: –0.19 to 0.06) mm/year. At baseline, fast progressors had a higher AL (23.40 ± 0.84 mm vs. 22.92 ± 0.80 mm, $P < .001$), lower spherical equivalent (SE) (–0.26 ± 1.54 vs. 1.00 ± 1.30, $P < .001$), higher horizontal RPR (–0.61 ± 2.01 vs. –1.65 ± 1.75, $P < .001$), and higher vertical RPR (–0.10 ± 2.12 vs. –0.79 ± 1.85, $P < .001$). (Figure 5) Additionally, fast progressors were more often female (58.46% vs 48.07%, $P = .003$) and of non-European ancestry (34% vs 21%, $P = .004$) (Table 3).

Ordinal regression, corrected for baseline AL, baseline refractive error category, ethnicity, sex, age, horizontal and vertical retinal curvature, revealed that faster AL progression was associated with higher horizontal RPR (OR: 1.27, CI: 1.16-1.41) and vertical RPR (OR: 1.35, CI: 1.24-1.47). Faster SE progression showed a similar yet weaker association (horizontal RPR:OR: 1.14, CI: 1.04-1.25; vertical RPR: OR: 1.12, CI: 1.02-1.22). A sensitivity analysis limited to participants with refractive errors between +0.5 and –0.5 diopters confirmed similar findings to the full cohort (horizontal RPR:OR: 1.18, CI: 1.04-1.34; vertical RPR: OR: 1.08, CI: 1.02-1.14). For the ROC analysis, we compared children in the highest and lowest quartiles of axial elongation, as this captures the most pronounced difference in progression. Additional comparisons across broader groupings (e.g., Q4 vs. Q1-Q3 and Q3 + Q4 vs. Q1 + Q2) are presented in the Supplementary Material.(Supplementary Figure 4). A univariate model with RPR (AUC = 0.66) had comparable predictive value to a model with baseline AL alone (AUC = 0.67). Combining RPR and AL increased the predictive value (AUC 0.67 vs. AUC 0.71). Adding covariates sex, age ethnicity and retinal curvature further increased predictive value (AUC 0.77).The predictive value of horizontal RPR was slightly higher than that of vertical RPR (Figure 6).

• **INCIDENT MYOPIA:** Of 962 children without myopia at baseline, 214 (22.2%) developed incident myopia between ages 9 and 14 years. Logistic regression, adjusted for follow up time, age, sex, ethnicity, retinal curvature and baseline AL, indicated a significantly increased risk of incident myopia for each diopter increase in horizontal RPR (OR: 1.40, CI: 1.21-1.64) and vertical RPR (OR: 1.29, CI: 1.12-1.50). Other factors that increased the risk of developing myopia were female gender (OR:1.89, CI:1.34-2.68) and longer axial length (mm) (OR:1.67, CI:1.28-2.19). AUC for inci-

TABLE 3. Myopia Progression Quartile Demographics.

	Quartiles of Axial Length Progression			
	Q1 (N = 337)	Q2 (N = 336)	Q3 (N = 336)	Q4 (N = 337)
Mean age, years	9.93 ± 0.41	9.88 ± 0.31	9.94 ± 0.40	9.92 ± 0.40
Girl (%)	48.07% (162)	50.00%(168)	52.08%(175)	58.46%(197)*
European (%)	79% (266)	71% (240)	74 % (249)	66% (222)*
ΔAL (mm/year)	0.04 ± 0.02	0.07 ± 0.01**	0.11 ± 0.01**	0.21 ± 0.07**
ΔSE (D/year)	−0.07 ± 0.30	−0.13 ± 0.28*	−0.17 ± 0.30**	−0.34 ± 0.25**
Spherical equivalent (D)	1.00 ± 1.30	1.04 ± 0.89	0.78 ± 1.08*	−0.26 ± 1.54**
Axial length (mm)	22.92 ± 0.80	22.96 ± 0.72	23.09 ± 0.74*	23.40 ± 0.84 **
Horizontal RPR 50	−1.65 ± 1.75	−1.86 ± 1.76	−1.73 ± 1.98	−0.61 ± 2.01**
Vertical RPR 50	−0.79 ± 1.85	−1.03 ± 1.86	−1.06 ± 1.92	−0.10 ± 2.12**

Significance testing was done using ANOVA with post hoc tukey analysis comparing measure to Q1 or Chi square test.
*$P < .05$.
**$P < .001$.

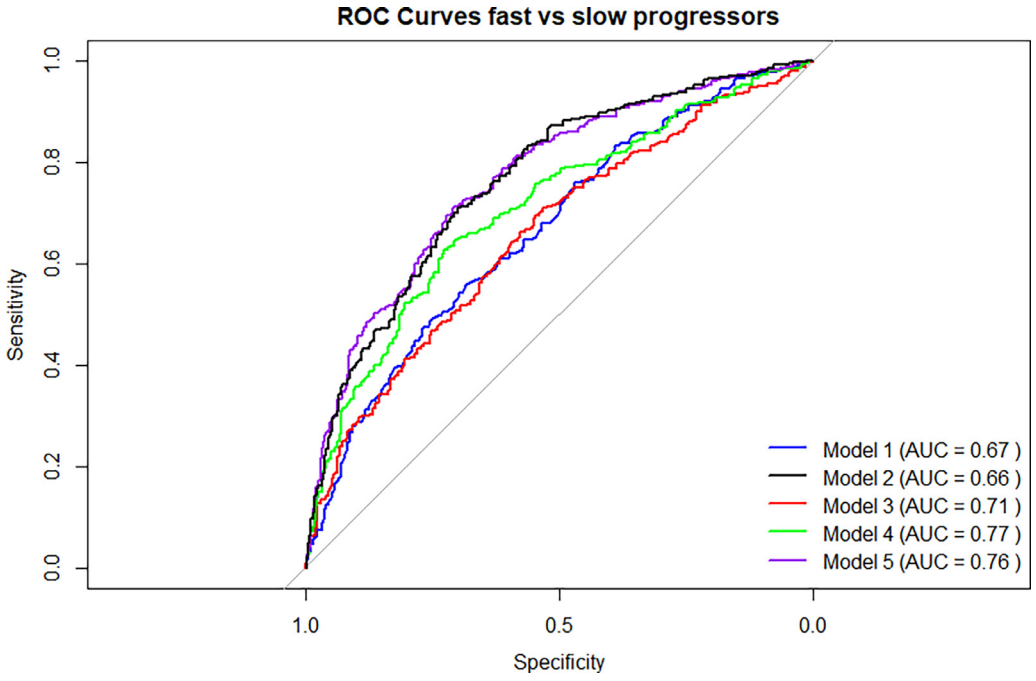

FIGURE 6. ROC curve for prediction of fast axial length progressors based on baseline RPR. Model 1: AL; Model 2: RPR; Model 3: AL+RPR; Model 4: Model 3 +retinal curvature+ age+ sex+ ethnicity; Model 5: vertical RPR+ covariates.

dent myopia was 0.67 for horizontal RPR and 0.66 for vertical RPR.

DISCUSSION

This study used an innovative design to investigate the relationships between peripheral refraction profiles, myopia progression, and incident myopia in a large cohort of children as they were followed from ages 9 to 13 years. We generated individualized peripheral refractive error profiles by combining ray-tracing simulations with an MRI-based personalized eye model. Our findings not only demonstrate the feasibility of using ray tracing for large-scale myopia research but also provide evidence that both vertical and horizontal relative peripheral refraction (RPR) are significantly associated with faster AL progression and a higher risk of incident myopia. Moreover, the predictive value of RPR is comparable to that of AL, and combining these measures

improves predictive accuracy. Our results reinforce the critical role of peripheral refraction in myopia progression, confirming its potential as target for intervention.

The MRI data revealed significant variation in both horizontal and vertical retinal radii with SD 1 mm. This anatomical difference resulted in clinically relevant variations in peripheral refraction, exceeding 8D between children with similar axial length and central SE. (Figure 3) This finding highlights that axial length and central SE alone are insufficient to determine whether a subject has a hyperopic or myopic RPR. Most optical interventions employ a standardized positive-powered defocus zone based on central refractive error.[10] However, our data suggest that defocus strategies may need to be individualized to optimize treatment outcomes. The anatomical variability in retinal curvature may explain the inconsistent results of optical intervention studies.

Our finding that myopic children exhibit more hyperopic relative peripheral refraction is consistent with previous studies on this topic.[8,9] However, these studies had not provided longitudinal evidence that peripheral hyperopia accelerates myopia progression or increases the likelihood of developing myopia.[9,12,13] Most studies typically measure peripheral refractive error by an autorefractor using a peripheral fixation target or a rotating arm around an axis passing through the eye's center-of- rotation, methods that present challenges and must be interpreted with caution.[14] Atchinson and Rozema emphasized the need to consider retinal shape, corneal curvature, axial length, and lens shape for an accurate assessment of peripheral refractive error.[14] To address these factors, we integrated MRI-derived retinal shape data with measurements of axial length, corneal curvature, and spherical equivalent to create personalized eye-models. An autorefractor, as it is a device developed to perform on-axis measurements, can only estimate refractions at maximum 30°eccentricity. Our approach provides a continuous range of eccentricities and enables measurements far beyond 30°. Our data reveal that differences in RPR between refractive error groups become more pronounced at high eccentricities. Furthermore, RPR at high eccentricities was more strongly associated with myopia progression, underscoring the importance of incorporating a large part of retinal anatomy when studying or targeting peripheral refraction.

Clinically, the results reflect on the effect of optical interventions, such as orthokeratology, multifocal spectacle lenses, dual-focus and multi-focus contact lenses and, more recently, spectacles with DIMS, HALT, and DOT design. These interventions have demonstrated significant efficacy in prevention of myopia and its progression by altering peripheral refraction.[10,41] A common feature among them is their ability to induce a relative peripheral myopic defocus while maintaining optimal central correction.[41-43] However, in a living systematic review from Lawrenson et al. uncertainty of sustained effects was an important conclusion, confirming the need for more and longer studies targeting RPR.[41] The proposed ray tracing techniques offer a novel way to assess the effect of these optical interventions on the retina at the individual level. By tracing the paths of light through different lenses and eye structures, this approach can predict how optical interventions may alter defocus in the periphery. Furthermore, by incorporating a person's retinal shape into the analysis, ray tracing may provide a more precise prediction of how these interventions slow down myopic growth.

• **STRENGTHS AND LIMITATIONS:** This study has some important strengths. First, the use of ray tracing overcomes many pitfalls that are encountered by commonly used measures of peripheral refraction.[14] Notably, this is the first study to apply ray tracing in a large cohort of children, children who were at a very susceptible age for developing myopia. Additionally, our approach allowed for the analysis of both the horizontal and the vertical meridian, as well as eccentricities in the far periphery. Second, the use of longitudinal data enabled us to track changes over time and identify prognostic factors associated with eye growth. Despite these strengths, the study does have some limitations. The MRI scans used had an isotropic resolution of 1 mm, potentially affecting the precision of retinal measurements. However, by fitting ellipses through data points obtained from multiple voxels, we partially mitigated this limitation. The correlation between axial length measured by IOL master and vitreous chamber depth measured by MRI was 0.86, indicating strong agreement.[26] The remaining imprecision is independent of retinal geometry or refractive error of the study participant; therefore, it is not likely to have introduced bias and affect comparisons between groups. Another limitation is that the RPR measurements cannot be validated against other methods as data for comparison are not available. Nevertheless, ray tracing methodology is well-established in refractive surgery, which supports its reliability.[19] Lastly, as most cohorts, our study had fixed times between visits, limiting our ability to determine the exact time of myopia onset.

CONCLUSION

Using advanced ray tracing techniques in a large longitudinal cohort of children, this study provides strong evidence for the role of RPR in myopia progression. We found that higher RPR is strongly associated with both faster axial length growth and increased risk of developing myopia. We also found a high variability of RPR between individuals, which may be of importance for optical interventions aimed at reducing myopia progression. While validation against standard clinical measurements is awaited, our findings affirm the relevance of RPR in predicting myopia progression

and can guide future efforts in developing targeted therapies.

DECLARATION OF GENERATIVE AI AND AI-ASSISTED TECHNOLOGIES IN THE WRITING PROCESS

During the preparation of this work the author(s) used OpenAI's GPT-4o in order to improve the readability and language of this manuscript. This assistance was solely used for linguistic enhancements and did not influence the research content, analysis, interpretation of data, or scientific conclusions. After using this tool/service, the author(s) reviewed and edited the content as needed and take(s) full responsibility for the content of the publication.

CREDIT AUTHORSHIP CONTRIBUTION STATEMENT

Sander C.M. Kneepkens: Writing – review & editing, Writing – original draft, Visualization, Methodology, Formal analysis, Data curation, Conceptualization. **Luc Van Vught:** Writing – review & editing, Software, Methodology, Formal analysis. **Jan Roelof Polling:** Writing – review & editing, Supervision, Conceptualization. **Caroline C.W. Klaver:** Writing – review & editing, Supervision, Resources, Project administration, Methodology, Funding acquisition, Conceptualization. **J. Willem L. Tideman:** Writing – review & editing, Validation, Supervision, Methodology, Data curation. **Jan-Willem M. Beenakker:** Writing – review & editing, Software, Resources, Methodology, Formal analysis, Conceptualization.

Funding/Support: This study received no funding. **Financial Disclosures:** The Generation R study is made possible by financial support from the Erasmus Medical Center, Rotterdam, the Netherlands; the Netherlands Organization for Scientific Research (NWO); the Netherlands Organization for Health Research and Development (ZonMw); the Dutch Ministry of Education, Culture and Science; the Dutch Ministry of Health, Welfare, and Sports; the European Commission (DG XII), Oogfonds, Stichting voor Ooglijders, Stichting voor Blindenhulp, Henkes Stichting, and Landelijke Stichting voor Blinden en Slechtzienden (LSBS). The research was funded by the European Research Council (ERC) under the European Union's Horizon 2020 research and innovation programme (ERC Advanced grant 101098324 to C.C.W.K.). and the Netherlands Organization for Scientific Research (NWO, grant 91815655). The author was sponsored by VISIA Imaging (22022021). The funding organizations had no role in the design or conduct of this research. They provided unrestricted grant.

REFERENCES

1. Holden BA, Fricke TR, Wilson DA, et al. Global prevalence of myopia and high myopia and temporal trends from 2000 through 2050. *Ophthalmology*. 2016;123:1036–1042.
2. Holden BA, Wilson DA, Jong M, et al. Myopia: a growing global problem with sight-threatening complications. *Community Eye Health*. 2015;28:35.
3. Wu P-C, Chang L-C, Niu Y-Z, Chen M-L, Liao L-L, Chen C-T. Myopia prevention in Taiwan. *Annals of Eye Science*. 2018;3:12.
4. Lam CS-Y, Lam C-H, Cheng SC-K, Chan LY-L. Prevalence of myopia among Hong Kong Chinese schoolchildren: changes over two decades. *Ophthalmic and Physiological Optics*. 2012;32:17–24.
5. Williams KM, Verhoeven VJ, Cumberland P, et al. Prevalence of refractive error in Europe: the European Eye Epidemiology (E(3)) Consortium. *Eur J Epidemiol*. 2015;30:305–315.
6. Németh J, Tapasztó B, Aclimandos WA, et al. Update and guidance on management of myopia. European Society of Ophthalmology in cooperation with International Myopia Institute. *Eur J Ophthalmol*. 2021;31:853–883.
7. Hoogerheide J, Rempt F, Hoogenboom WP. Acquired myopia in young pilots. *Ophthalmologica*. 1971;163:209–215.
8. Sng CCA, Lin X-Y, Gazzard G, et al. Peripheral refraction and refractive error in Singapore Chinese children. *Invest Ophthalmol Visual Sci*. 2011;52:1181–1190.
9. Atchison DA, Li SM, Li H, et al. Relative peripheral hyperopia does not predict development and progression of myopia in children. *Invest Ophthalmol Vis Sci*. 2015;56:6162–6170.
10. Jonas JB, Ang M, Cho P, et al. IMI prevention of myopia and its progression. *Invest Ophthalmol Visual Sci*. 2021;62(5):6.
11. Papadogiannis P, Börjeson C, Lundström L. Comparison of optical myopia control interventions: effect on peripheral image quality and vision. *Biomed Opt Express*. 2023;14:3125–3137.
12. Lee TT, Cho P. Relative peripheral refraction in children: twelve-month changes in eyes with different ametropias. *Ophthalmic Physiol Opt*. 2013;33:283–293.
13. Mutti DO, Sinnott LT, Mitchell GL, et al. Relative peripheral refractive error and the risk of onset and progression of myopia in children. *Invest Ophthalmol Visual Sci*. 2011;52:199–205.
14. Atchison DA, Rozema JJ. Technical notes on peripheral refraction, peripheral eye length and retinal shape determination. *Ophthalmic Physiol Opt*. 2023;43:584–594.
15. Fedtke C, Ehrmann K, Holden BA. A review of peripheral refraction techniques. *Optom Vis Sci*. 2009;86:429–446.
16. Haasjes C, Vu THK, Beenakker J-WM. Patient-specific mapping of fundus photographs to three-dimensional ocular imaging. *Med Phys*. 2025;52(4):2330–2339.
17. van Vught L, Que I, Luyten GPM, Beenakker JM. Effect of anatomical differences and intraocular lens design on negative dysphotopsia. *J Cataract Refract Surg*. 2022;48:1446–1452.
18. van Vught L, Shamonin DP, Luyten GPM, Stoel BC, Beenakker JM. MRI-based 3D retinal shape determination. *BMJ Open Ophthalmol*. 2021;6:e000855.
19. van Vught L, Luyten GPM, Beenakker JM. Distinct differences in anterior chamber configuration and peripheral aberrations in negative dysphotopsia. *J Cataract Refract Surg*. 2020;46:1007–1015.

20. Verkicharla PK, Suheimat M, Schmid KL, Atchison DA. Peripheral refraction, Peripheral eye length, and retinal shape in myopia. *Optometry Vision Sci*. 2016;93:1072–1078.
21. Savini G, Hoffer KJ, Kohnen T. IOL power formula classifications. *J Cataract Refract Surg*. 2024;50:105–107.
22. van Vught L, Haasjes C, Beenakker JWM. ZOSPy: optical ray tracing in Python through OpticStudio. *J Open Source Software*. 2024;9(96):5756.
23. Simpson MJ. Optical modeling of the entire visual field of the eye. *J Opt Soc Am A*. 2023;40:D7–D13.
24. Olsen T, Hoffmann P. C constant: new concept for ray tracing-assisted intraocular lens power calculation. *J Cataract Refract Surg*. 2014;40:764–773.
25. Canovas C, Artal P. Customized eye models for determining optimized intraocular lenses power. *Biomed Opt Express*. 2011;2:1649–1662.
26. Kneepkens SCM, Marstal K, Polling JR, et al. Eye size and shape in relation to refractive error in children: a magnetic resonance imaging study. *Invest Ophthalmol Vis Sci*. 2023;64:41.
27. Jaarsma-Coes MG, Ferreira TA, Marinkovic M, et al. Comparison of Magnetic resonance imaging-based and conventional measurements for Proton beam therapy of Uveal melanoma. *Ophthalmol Retina*. 2023;7:178–188.
28. Pope JM, Verkicharla PK, Sepehrband F, Suheimat M, Schmid KL, Atchison DA. Three-dimensional MRI study of the relationship between eye dimensions, retinal shape and myopia. *Biomed Opt Express*. 2017;8:2386–2395.
29. Jaddoe VW, van Duijn CM, Franco OH, et al. The Generation R Study: design and cohort update 2012. *Eur J Epidemiol*. 2012;27:739–756.
30. Kooijman MN, Kruithof CJ, van Duijn CM, et al. The Generation R Study: design and cohort update 2017. *Eur J Epidemiol*. 2016;31:1243–1264.
31. Beenakker J-WM, Shamonin DP, Webb AG, Luyten GPM, Stoel BC. Automated retinal topographic maps measured with magnetic resonance imaging. *Invest Ophthalmol Visual Sci*. 2015;56:1033–1039.
32. van Vught L, Dekker CE, Stoel BC, Luyten GPM, Beenakker J-WM. Evaluation of intraocular lens position and retinal shape in negative dysphotopsia using high-resolution magnetic resonance imaging. *J Cataract Refract Surg*. 2021;47:1032–1038.
33. Escudero-Sanz I, Navarro R. Off-axis aberrations of a wide-angle schematic eye model. *J Opt Soc Am A*. 1999;16:1881–1891.
34. Li Q, Fang F. Physiology-like crystalline lens modelling for children. *Opt Express*. 2020;28:27155–27180.
35. Uhlhorn SR, Borja D, Manns F, Parel J-M. Refractive index measurement of the isolated crystalline lens using optical coherence tomography. *Vision Res*. 2008;48:2732–2738.
36. Escudero-Sanz I, Navarro R. Off-axis aberrations of a wide-angle schematic eye model. *J Opt Soc Am A Opt Image Sci Vis*. 1999;16:1881–1891.
37. van Vught L, Haasjes C, Beenakker J-WM. ZOSPy: optical ray tracing in Python through OpticStudio. *J Open Source Software*. 2024;9:5756.
38. Centraal Bureau voor deStatistiek. *Voorburg/Heerlen: Centraal Bureau voor de Statistiek*. Allochtonen in Nederland 2004 (Kengetal: B-52); 2004.
39. Hajian-Tilaki K. Receiver operating characteristic (ROC) curve analysis for medical diagnostic test evaluation. *Caspian J Intern Med*. 2013;4:627–635.
40. Kim JH. Multicollinearity and misleading statistical results. *Korean J Anesthesiol*. 2019;72(6):558–569.
41. Lawrenson JG, Shah R, Huntjens B, et al. Interventions for myopia control in children: a living systematic review and network meta-analysis. *Cochrane Database Syst Rev*. 2023;2(2):CD014758.
42. Queirós A, Amorim-de-Sousa A, Lopes-Ferreira D, Villa-Collar C, Gutiérrez ÁR, González-Méijome JM. Relative peripheral refraction across 4 meridians after orthokeratology and LASIK surgery. *Eye Vision*. 2018;5:1–8.
43. Kang P, Swarbrick H. New perspective on myopia control with orthokeratology. *Optometry Vision Sci*. 2016;93:497–503.